IJRCS

International Journal of Robotics and Control Systems
Vol. 5, No. 3, 2025, pp. 1790-1807
ISSN 2775-2658
http://pubs2.ascee.org/index.php/ijrcs

ASCEE

Improved of Sliding Mode Control for Maximum Power Point Tracking in Solar Photovoltaic Applications Under Varying Conditions

Alaq F. Hasan [a,1], Mohanad Nawfal [b,2], Ahmed S. Al-Araji [b,3], Huthaifa Al-Khazraji [b,4,*], Amjad J. Humaidi [b,5]

[a] Technical Engineering College, Middle Technical University, Baghdad, Iraq
[b] College of Control and System Engineering, University of Technology-Iraq, Baghdad, Iraq
[1] alaaqf.hasan@mtu.edu.iq; [2] 60158@uotechnology.edu.iq; [3] 60166@uotechnology.edu.iq;
[4] 60141@uotechnology.edu.iq; [5] amjad.j.humaidi@uotechnology.edu.iq
* Corresponding Author

ARTICLE INFO

Article history
Received May 12, 2025
Revised June 26, 2025
Accepted July 30, 2025

Keywords
Solar Photovoltaic (PV);
Maximum Power Point Tracking;
Synergetic Algorithm Control;
Sliding Mode Controller

ABSTRACT

The solar energy generation sector has received widespread interest compared to other types of sustainable energy generation. This is owing to its high efficiency and the availability of environmental factors essential to the operation of these systems in various parts of the world. However, increased the power extracted from these systems are a critical issue as their conversion efficiency is low. Therefore, a maximum power point tracking (MPPT) controller is necessary in a photovoltaic generation system (PV) for maximum power extraction. This study aims to explore the performance of the MPPT system that uses an improved sliding mode controller (SMC) to identify and track a maximum power point (MPP) of a PV system and compares it to synergetic algorithm control (SACT). To implementing this purpose, MATLAB/Simulink model of a stand-alone PV panel is developed. Then, the analysis of the performance efficiency of the PV system based on the proposed MPPT methods are implemented under varying environmental conditions. Being able to track the MPP perfectly in the case of a sudden change in environment conditions, the improved SMC is proven by the results to be superior in stabilizing the boost converter's operation, leading to enhanced PV system stability. This has led to a reduction in power losses and an increase in efficiency.

1. Introduction

The urgent need to reduce the adverse effects of climate change has led to the development and improvement of sustainable energy technologies. Amongst these technologies, photovoltaic (PV) systems have been classified as a leading technology in the field of sustainable energy because of their ability to directly convert solar radiation into electricity. Solar energy provides a reliable and non-toxic source of energy that can significantly reduce our dependence on coal, oil and natural gas, thereby helping to reduce the rising levels of carbon dioxide in the atmosphere [1]-[4]. Nonetheless, enhancing the efficiency of PV systems remains a fundamental challenge, as their production rate depends on environmental variables such as solar irradiance and temperature,

which, in turn, are characterized by their continuous volatility during the day or season. The point at which the system produces the highest possible power is known as the Maximum Power Point (MPP). Determining and keeping track of this critical point is essential for enhancing the overall efficiency and energy yield of PV systems, particularly in areas where environmental conditions oscillate rapidly. The variation in the value of the solar irradiance and temperature often leads to inefficient energy generation, this demands the use of sophisticated control strategies to ensure that PV systems operate at their MPP [5].

Control algorithm strategies have been successfully designed for improving wide range of systems [6]-[18]. In the context of PV systems, the objective of the controller is to improve the performance of the MPPT in order to dynamically update the operating point of a PV system to ensure that it reliably generates the maximum power under changing environmental conditions. Throughout the years, numerous MPPT techniques have been formulated and applied, with different advantages and disadvantages depending on application context and natural surroundings. Some of the MPPT techniques depended on pre-calculated or estimated value of the photovoltaic panel parameters to synthesize the control signal required to drive the photovoltaic panel to its MPP as in [19], Pratima Das proposed an open circuit voltage method as MPPT where the MPP voltage (V_{mpp}) is estimated as a segment of the measured open circuit voltage (V_{oc}). In [20], J.S. Kumari et al. used the short circuit current (SCC) method for improving the MPPT performance in solar models. The SCC method for MPPT in PV systems estimates the MPP current (I_{mpp}) as a fixed fraction (around 85-95%) of the short circuit current (I_{SC}).

Other types of the MPPT techniques used the real-time photovoltaic (PV) voltage and current to track the MPP as in [21], R. S. Sharma and P. K. Katti utilized the MPPT based Perturb & Observation algorithm (P&O). The main concept of P&O is to continuously change the operating voltage of the PV system and observe the resulting changes in the extracted power to find the MPP. The disadvantage of this algorithm is oscillation around MPP. Since the system continuously perturbs the voltage, it doesn't settle exactly at the MPP but oscillates around it, causing small power losses. In [22], D. Guiza et al. employed a modified P&O algorithm to reduce the effect of oscillatory behavior near the MPP on the produced power and advance the speed of tracking. The main idea of this modified algorithm is based on the contrast between dP/dV and a specified error. The algorithm determines the subsequent step of the control signal, if the real-time power is distant from the MPP, the algorithm produces a large step value. Otherwise, it generates a small step value. In [23], R. I. Putri et al. utilized an incremental conductance method to enhance the overall performance of the PV system. The method works by comparing the incremental conductance ($\Delta I/\Delta V$) to the instantaneous conductance (I/V) of the PV module. The results of this method were compared with the P&O algorithm in this work and the simulation results show, that the IC method had better performance and lower oscillation. In [24], H. Yau and C. Wu offered adaptive MPPT technical built upon the extremum seeking control (ESC) method to improve the performance of PV system. The ESC method uses real-time feedback and control techniques to continuously optimize the MPP without relying on a predefined model of the PV system or environmental conditions.

In [25], P. Cheng et al. suggested a fuzzy logic control (FLC) technique for improving the MPPT performance in PV systems. The main idea of FLC as an MPPT method is to track the MPP by using linguistic rules to manage the nonlinear and dynamic characteristics of PV systems under varying environmental conditions like irradiance and temperature. To optimize the performance of the suggested approach, the authors used the particle swarm optimization algorithm to optimize the setting values of the input members' functions. In [26], K. Kayisli presented super twisting sliding mode-type-2 fuzzy MPPT control to achieve optimal tracking for MPP of the PV system. The fundamental concept of SMC as MPPT technique is to force the PV system to slide along a sliding surface in the control space, ensuring that it continuously operates at the MPP under varying conditions like irradiance and temperature changes. The disadvantage with SMC using is chattering phenomenon, which define as a high-frequency oscillation around the sliding surface as a result of

the switching nature of the control. To diminish the chattering problem, the author suggested the super-twisting algorithm based on type-2 fuzzy set.

Last type of MPPT techniques employs dual loops for MPP tracking. The external loop is used for real-time maximum power estimation by identifying the voltage at MPP, while the internal loop uses this estimate voltage as a setpoint and generates an appropriate control action to optimize the PV system for operation at the estimated MPP. Dahech et al. [27] proposed a backstepping sliding mode control (BSMC) to enhance the performance of MPPT in order to enable the effective operation of the PV systems in the face of varying external conditions. In this approach, constant voltage controller method is used maintain a constant voltage difference (V_{mpp}) across the photovoltaic panel. Moreover, the internal loop employs a BSMC to stabilize the PV system at the estimated reference V_{mpp}. Kihal et al. [28] employed an adaptive integral derivative sliding mode control (AIDSMC) to enhance the PV system's capability. In this approach, the P&O algorithm, which is employed to generate the reference voltage for MPPT's internal loop, is combined with the external voltage control mechanism formulated using an AIDSMC. The obtained findings with the presented MPPT indicate remarkable dynamic performance under rapid changes in irradiation.

The sliding mode control and the synergetic control are novel control strategies that focus on controlling and managing intricate systems. However, they have major contrasts in design methodology, and implementation. The sliding mode control strategy is based on variable structure control, where the system's states are driven to attain a predefined sliding manifold and then remain constrained to this manifold by using a discontinuous switching term [29]-[32]. On the other hand, the synergetic control strategy allows the system's states to evolve along predefined invariant manifolds set by the designer during the attainment of intended performance, even under the influence of external disturbances [33]-[35]. The following is a concise summary of the work's contribution:

1. Design and implement two MPPT methods represented in sliding mode control and synergetic control to evaluate and follow the MPP of the PV panel.
2. Executing a comparative evaluation between these two control methods in terms of tracking efficiency and oscillation around MPP.

The remainder of this paper is divided into seven sections, which are arranged in the following manner: Section 2 describes the mathematical models of the photovoltaic power source. Section 3 contains the design of the synergetic algorithm control theory as MPPT technique. In Section 4, the design of the sliding mode controller as MPPT technique is presented. Section 5 provides the simulation results using MATLAB software and comparison results. Finally, in Section 6, the conclusions are drawn.

2. Mathematical Model

The photovoltaic generation system is structured with multiple components, comprising a PV module, a DC-DC boost converter, a controller, and a load. Fig. 1 illustrates a typical photovoltaic generation system with an MPPT algorithm. The photovoltaic module serves as the core of system. The power extracted from a PV system is influenced by environmental factors such as solar irradiation and temperature, which fluctuate throughout the operational periods. These fluctuations impart nonlinear characteristics to the system. Therefore, employing an MPPT controller is essential for a PV system. The MPPT controller's aim is to optimize power extraction by continuously adjusting the electrical operating point of the modules. DC-DC boost converters are commonly employed in PV systems to step up the voltage while regulating power flow [36]-[37].

2.1. Modeling of Photovoltaic Cell

The PV cell functions to convert sunlight into electricity. The circuit of the PV cell under investigation, representing a stand-alone PV plant [38], is shown in Fig. 2. It includes the current

generated by the cell due to sunlight (I_{ph}), the p-n junction of the PV cell, the series resistance (R_s), which accounts for the resistance within the cell due to electron movement through the material, and the shunt resistance (R_{sh}), which represents the leakage current path within the cell. The relationship between the PV cell variables is described by the following equation [39]:

$$I_{pv} = I_{ph} - I_o\left(\exp\frac{q(V_{pv} + R_s I_{pv})}{nN_s KT} - 1\right) - I_{sh} \quad (1)$$

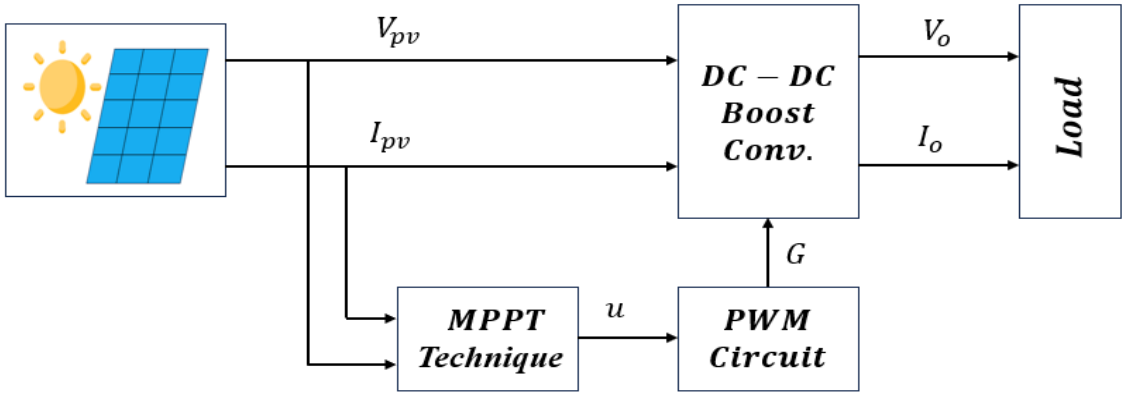

Fig. 1. Photovoltaic generation system with MPPT algorithm

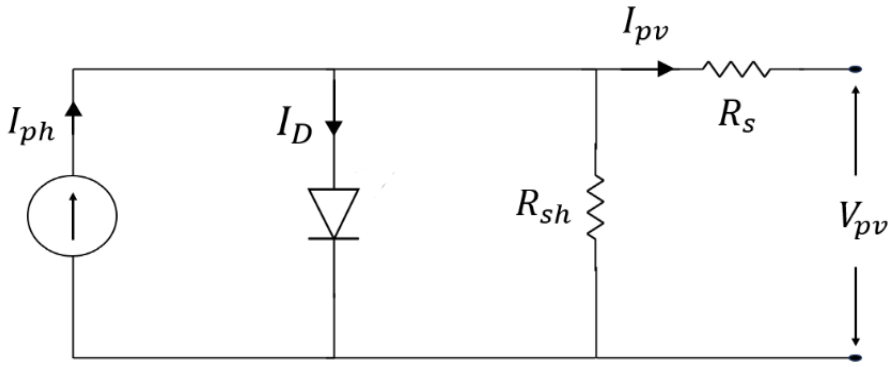

Fig. 2. The equivalent circuit of photovoltaic cell

where I_{pv} is the PV cell current, V_{pv} is the PV cell voltage, I_{ph} is the photocurrent (current generated by sunlight), I_o is the saturation current of the diode, n is the ideality factor of the diode (1.6), N_s Number of cells in series (36), q is the charge of an electron ($1.6 * 10^{-19}$ C), T is the operating temperature of the panel (in Kelvin), and k is Boltzmann's constant ($1.38 * 10^{-23}$J/K). I_{ph} is defined as:

$$I_{ph} = (I_{sc} + k_i(T - T_n))\frac{G}{G_n} \quad (2)$$

where k_i is the short circuit current temperature coefficient (0.0032), I_{sc} is the short circuit current, G_n solar irradiation in STC (1000 W/m^2), T_n is the reference temperature (25 °C), and G irradiation level in W/m^2. The mathematical expression for the saturation diode current I_o is given in the following equation [40]:

$$I_o = I_{rs}\left(\frac{T}{T_n}\right)^3 \exp\left[\frac{qE_g}{nk}\left(\frac{1}{T_n} - \frac{1}{T}\right)\right] \quad (3)$$

where E_g is the energy band-gap (1.1eV), and the reverse saturation diode current I_{rs} is:

$$I_{rs} = I_{sc}/(\exp\left(\frac{qV_{oc}}{nN_skT}\right) - 1) \tag{4}$$

where V_{oc} is the open circuit voltage. Finaly, the shunt current is:

$$I_{sh} = \frac{V_{pv} + R_sI_{pv}}{R_{sh}} \tag{5}$$

These equations are modeled in MATLAB using the specifications of the MSX 60W PV panel [41]. The characteristic curves of the panel under varying levels of solar irradiance and temperature are illustrated in Fig. 3 and Fig. 4.

2.2. Model of DC-DC Boost Converter

There are numerous types of DC-DC converter circuits that are capable of being utilized with PV systems. The most widely used converter is the step-up converter (boost DC-DC converter) due to its high efficiency and ease of implementation. The DC-DC boost converter's equivalent circuit is illustrated in Fig. 5. This converter operates by transforming the DC voltage input to a higher level. The mathematical analysis of the DC-DC boost converter is done based on the two operational modes of the circuit, where the operational mode of the circuit depends on whether the IGBT transistor gate is ON or OFF.

Accordingly, the mathematical expressions for the inductor current (I_L) and the output capacitor voltage (V_o) are as follows [42]:

$$\begin{cases} \frac{dI_L}{dt} = \frac{V_{pv} - V_o}{L} + \frac{V_o}{L}u \\ \frac{dV_o}{dt} = \frac{1}{C_o}(I_L - \frac{V_o}{R}) - \frac{I_L}{C_o}u \end{cases} \tag{6}$$

where u is the duty ratio, considered the control variable.

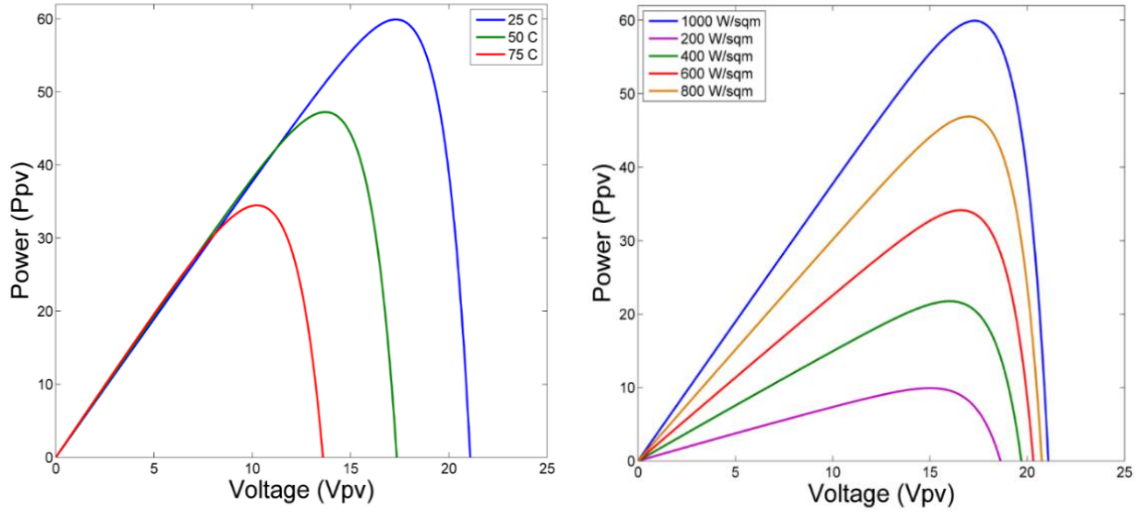

(a) (b)

Fig. 3. P-V characteristics of MSX 60W PV panel for (a) varying temperature (b) varying irradiance

By combining the two equations in Eq. (6) and assuming $I_L = I_{pv}$, the mathematical expressions of the DC-DC boost converter circuit can be written in the state-space representation as follows:

$$x = \begin{bmatrix} I_{pv} \\ V_o \end{bmatrix} \tag{7}$$

$$\dot{x} = f(x,t) + g(x,t)u = \begin{bmatrix} \frac{V_{pc} - V_o}{L} \\ \frac{I_{pv}}{C_o} - \frac{V_o}{RC_o} \end{bmatrix} + \begin{bmatrix} \frac{V_o}{L} \\ -\frac{I_{pv}}{C_o} \end{bmatrix} u$$

3. Design a Maximum Power Point Tracking Technique Based on a Synergetic Control Approach

The first step in the synergetic synthesis process design is identifying a macro variable function in terms of the system states [43]-[44].

$$\sigma = \sigma(x,t) \tag{8}$$

The macro variable (σ) can be identified by a customized function, $\sigma(x,t)$. The principal aim of the synergetic control approach is to propel the states of the system to work on the $\sigma = 0$ manifold, thereby defining the desired dynamics of the macro-variable evolution as follows [45]:

$$\lambda\dot{\sigma} + \sigma = 0 \tag{9}$$

The solution to the differential equation above can be obtained as follows:

$$\sigma(t) = \sigma_0 \, e^{-t/\lambda} \tag{10}$$

As shown in the previous equation, the macro-variable is attracted to zero from any initial condition (σ_0). The speed at which the system states settle at the manifold depends on the value of the design parameter λ [46].

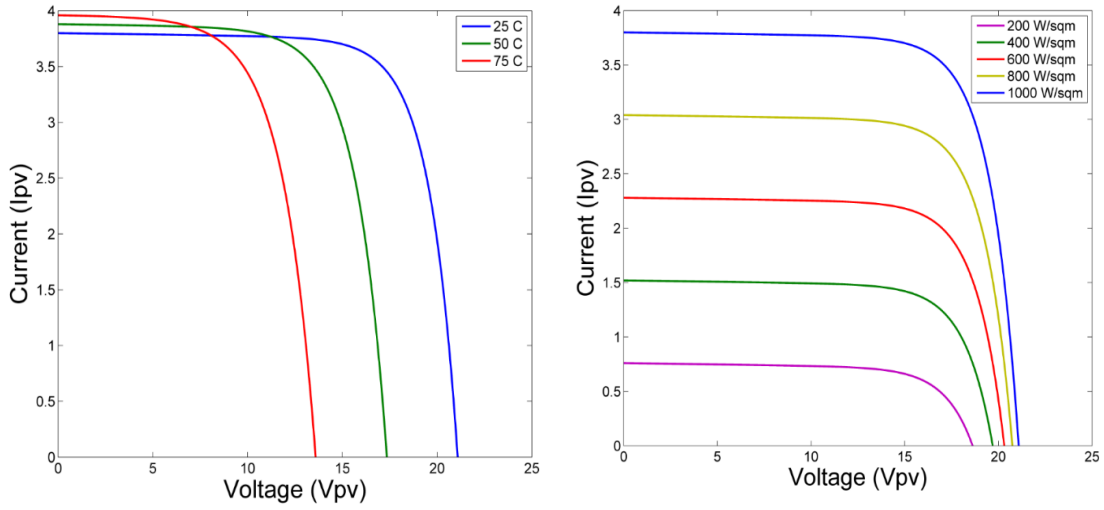

(a) (b)

Fig. 4. I-V characteristics of MSX 60W PV panel for (a) varying temperature (b) varying irradiance

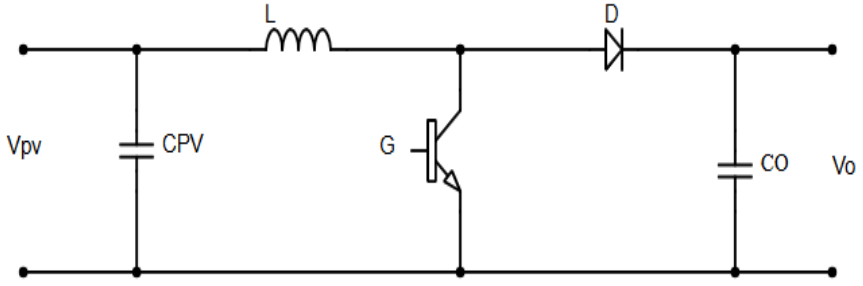

Fig. 5. The equivalent circuit of DC-DC boost converter

To ensure the photovoltaic generation system operates at the MPP, the following macro-variable is considered:

$$\sigma = \frac{\partial P_{pv}}{\partial V_{pv}} = I_{pv} + V_{pv}\frac{\partial I_{pv}}{\partial V_{pv}} \tag{11}$$

Taking the time derivative of the macro-variable results in

$$\begin{gathered}\dot{\sigma} = \frac{\partial \sigma}{\partial x}\frac{\partial x}{\partial t} = \frac{\partial \sigma^{T}}{\partial x}\ (f(x,t) + g(x,t)u) \\ \dot{\sigma} = \frac{\partial \sigma}{\partial I_{pv}}\left(\frac{V_{pc} - V_o}{L} + \frac{V_o}{L}u\right)\end{gathered} \tag{12}$$

Using Eqs. (11) and (12), we propose the following control action:

$$u = 1 - \frac{V_{pc}}{V_o} - \frac{\sigma}{\lambda\, b} \tag{13}$$

where

$$b = \frac{V_o}{L}\frac{\partial \sigma}{\partial I_{pv}} \tag{14}$$

To emphasize the stability of the PV system based on the SACT as the MPPT, the following Lyapunov function has been adopted:

$$V = \frac{1}{2}\sigma^2 \tag{15}$$

The time derivative of Eq. (15) gives:

$$\begin{gathered}\dot{V} = \sigma\dot{\sigma} \\ \dot{V} = \sigma\left(\frac{\partial \sigma}{\partial I_{pv}}\left[\frac{V_{pc} - V_o}{L} + \frac{V_o}{L}u\right]\right) \\ \dot{V} = -\frac{\sigma^2}{\lambda}\end{gathered} \tag{16}$$

It should be indicated that for all $t \geq 0$, V is positive definite, and $\dot{V}$ is negative definite, implying that the macro-variable σ will ultimately converge to zero as t approaches infinity

4. Design a Maximum Power Point Tracking Technique Based on Sliding Mode Control

The first step in the design of SMC is to define a sliding surface function, $s(x,t)$. The second step involves designing a control mechanism to drive and stabilize the system's states on the sliding surface [47]-[49]. Ensuring the system's states reach and remain on the sliding surface maximizes power extraction from the PV system. To achieve this, the following equation can be used to define the sliding surface:

$$s(x,t) = \frac{\partial P_{pv}}{\partial V_{pv}} = I_{pv} + V_{pv}\frac{\partial I_{pv}}{\partial V_{pv}} \tag{17}$$

The time derivative of sliding surface function is

$$\dot{s}(x,t) = \frac{\partial s}{\partial x}\frac{\partial x}{\partial t} = \frac{\partial s^T}{\partial x}\dot{x} = \begin{bmatrix} \frac{\partial s}{\partial I_{pv}} & \frac{\partial s}{\partial V_o} \end{bmatrix} \begin{bmatrix} \frac{dI_{pv}}{dt} \\ \frac{dV_o}{dt} \end{bmatrix} \tag{18}$$

As $\frac{\partial s}{\partial V_o} = 0$

$$\therefore \dot{s}(x,t) = \frac{\partial s}{\partial I_{pv}}\frac{dI_{pv}}{dt} = \frac{\partial s}{\partial I_{pv}}\left[\frac{V_{pc} - V_o}{L} + \frac{V_o}{L}u\right] \tag{19}$$

The control law is commonly divided into two major parts. The first one is denoted as "the equivalent control law", and it is found by setting the first derivative of the sliding surface function to zero. The second part, termed "the switching control law", ensures the controlled variable remains on the sliding surface.

$$u = u_{eq} + u_{sw} \tag{20}$$

By setting Eq. (20) to zero, the equivalent control law (u_{eq}) is determined as follows:

$$\frac{\partial s}{\partial I_{pv}}\left[\frac{V_{pc} - V_o}{L} + \frac{V_o}{L}u_{eq}\right] = 0 \tag{21}$$

$$u_{eq} = -\frac{\frac{V_{pc} - V_o}{L}}{\frac{V_o}{L}} = 1 - \frac{V_{pc}}{V_o} \tag{22}$$

In conventional SMC, the switching control law u_{sw} is typically defined as

$$u_{sw} = -k\,\mathrm{sign}(s) \tag{23}$$

where k is a design parameter, and the $\mathrm{sign}(s)$ function is defined as:

$$\mathrm{sign}(s) = \begin{cases} -1 & \text{if} \quad s < 0 \\ 0 & \text{if} \quad s = 0 \\ +1 & \text{if} \quad s > 0 \end{cases} \tag{24}$$

To alleviate the chattering problem caused by the presence of the $\mathrm{sign}(s)$ function, an approximated signum function is employed as a surrogate for the sign function [50].

$$\mathrm{sgn}(s) \approx \frac{2}{\pi}\tanh(\beta s) \tag{25}$$

where β is a design parameter. The control law is then formulated as

$$u = 1 - \frac{V_{pc}}{V_o} - \frac{2k}{\pi}\tanh(\beta s) \tag{26}$$

To emphasize the stability of the PV system based on the SMC as the MPPT, the following Lyapunov function has been adopted:

$$V = \frac{1}{2}s^2 \tag{27}$$

The time derivative of Eq. (28) gives [51]:

$$\dot{V} = s\dot{s} = s\left[\frac{\partial s}{\partial I_{pv}}\left(\frac{V_{pc} - V_o}{L} + \frac{V_o}{L}u\right)\right] \tag{28}$$

$$\dot{V} = s\left[\frac{\partial s}{\partial I_{pv}}\left(\frac{V_{pc}-V_o}{L}+\frac{V_o}{L}\left(1-\frac{V_{pc}}{V_o}-\frac{2k}{\pi}\tanh(\beta s)\right)\right)\right]$$

$$\dot{V} = s\frac{\partial s}{\partial I_{pv}}\frac{V_o}{L}\left[-\frac{2k}{\pi}\tanh(\beta s)\right]$$

$$\frac{\partial s}{\partial I_{pv}} = \frac{\partial}{\partial I_{pv}}\left(I_{pv}+V_{pv}\frac{\partial I_{pv}}{\partial V_{pv}}\right) = \frac{\partial I_{pv}}{\partial V_{pv}}\frac{\partial V_{pv}}{\partial I_{pv}} + V_{pv}\frac{\partial}{\partial I_{pv}}\left(\frac{\partial I_{pv}}{\partial V_{pv}}\right) \quad (29)$$

With some assumptions, Eq. (1) can be obtained

$$I_{pv} = I_{ph} - I_o\left(\exp\frac{qV_{pv}}{nN_sV_T} - 1\right) \quad (30)$$

The derivative of the I_{pv} equation with respect to V_{pv}:

$$\frac{\partial I_{pv}}{\partial V_{pv}} = -\frac{q}{nN_sV_T}I_D\exp\left(\frac{q}{nN_sV_T}\right) \quad (31)$$

Now, rearranging the $\frac{\partial I_{pv}}{\partial V_{pv}}$ with respect to V_{pv} yields,

$$V_{pv} = \frac{nN_sV_T}{q}\ln\left(\frac{I_D}{I_{ph}+I_D-I_{pv}}\right) \quad (32)$$

The $\frac{\partial I_{pv}}{\partial V_{pv}}$ equation can be rearranged again with respect to I_{pv} yielding,

$$\frac{\partial V_{pv}}{\partial I_{pv}} = -\frac{nN_sV_T}{q}\ln\left(\frac{I_D}{I_{ph}+I_D-I_{pv}}\right) \quad (33)$$

$$\frac{\partial s}{\partial I_{pv}} = \frac{1}{V_{pv}} - \frac{I_{pv}}{{V_{pv}}^2}\frac{\partial V_{pv}}{\partial I_{pv}} + \frac{q}{nN_sV_T}\frac{\partial I_{pv}}{\partial V_{pv}}\frac{\partial V_{pv}}{\partial I_{pv}} \quad (34)$$

Upon completing these steps, it was determined that the sign of $\frac{\partial s}{\partial I_{pv}}$ is always positive and guaranteeing the asymptotic stability of the PV system controlled by SMC.

5. Results and Discussion

The electrical characteristics of MXS 60W PV panel are listed in Table 1. A PV panel was created using MATLAB/Simulink, and the "Ode23t" solver was applied as a numerical solver. The corresponding value of controller parameter λ of the SACT is 6000 and the corresponding value of controller parameters k and β of the SMC is 0.09 and 0.6 respectively. The PV panel power, output power, and duty ratio of the MXS 60W PV panel simulated with the proposed MPPT methods under standard test conditions ($T = 25$ ℃ and $G = 1000\ W/m^2$) are shown in Fig. 6.

Table 1. Specifications of MXS 60W PV module [35]

Parameter	Value
The power at MPP	60 W
The current at MPP	3.5 A
The voltage at MPP	17.1 V
Short circuit current	3.8 A
Open circuit voltage	21.1 V

For dynamic analysis, the responses of the proposed MPPT methods were tested under varying solar irradiation in the range of $(600-1000)\ W/m^2$ at $T = 25$℃ and under varying temperature

in the range of $(25-50)\,℃$ at $G = 1000\,W/m^2$. The change in solar irradiation used in the examination of the proposed MPPT methods in the first test is depicted in Fig. 7. The PV panel power, load power, and duty ratio of the proposed MPPT methods are illustrated in Fig. 8. The variation in temperature used in the examination of the proposed MPPT methods in the second test is depicted in Fig. 9 while, the Fig. 10 shows the PV panel power, load power, and duty ratio under varying temperature conditions. The PV system's tracking efficiency can be evaluated using the following equation:

$$\eta = \left(\frac{P_{pv}}{P_{MPP}}\right) 100\% \tag{35}$$

where P_{MPP} represents the power at the MPP.

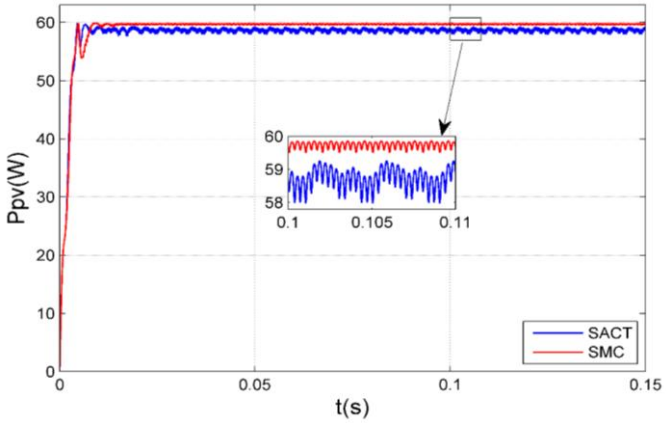

(a) The Power of PV panel

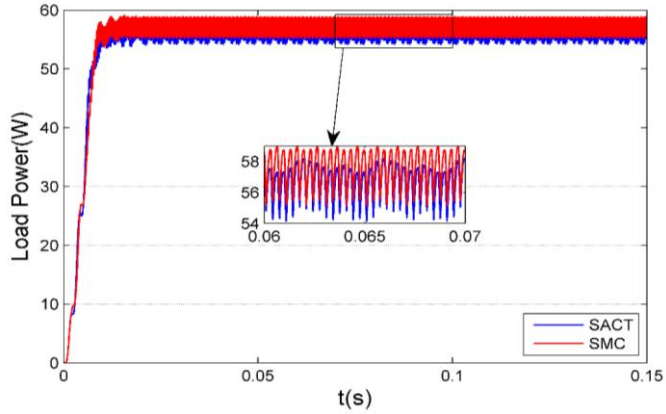

(b) Load power

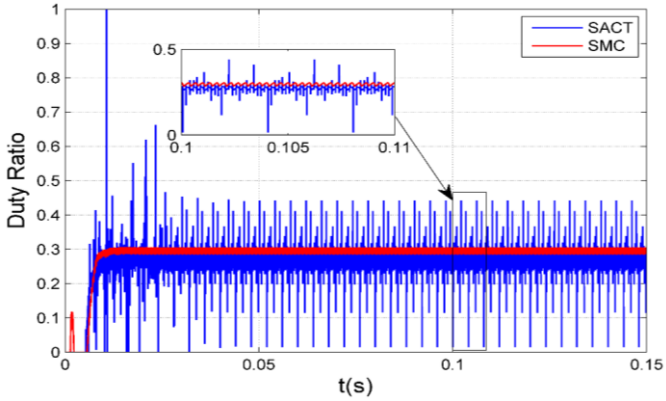

(c) Duty ratio

Fig. 6. Dynamic response of MPPT

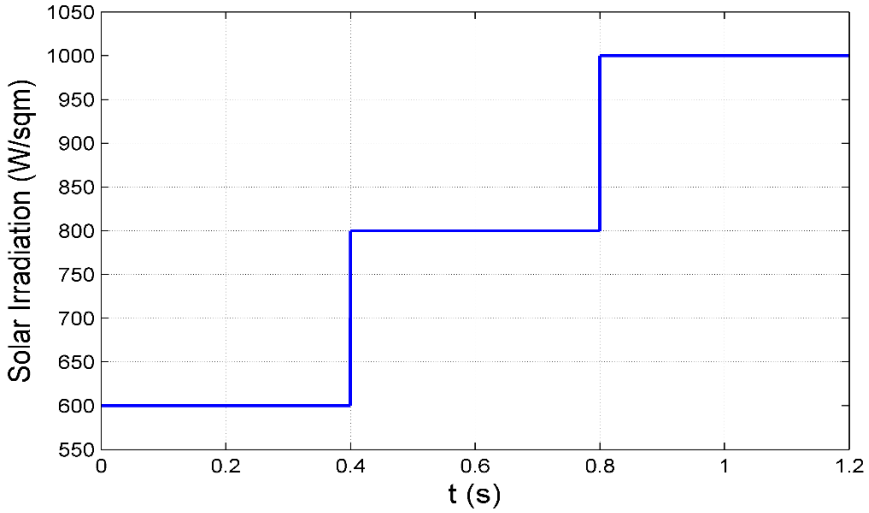

Fig. 7. Variation of irradiation level

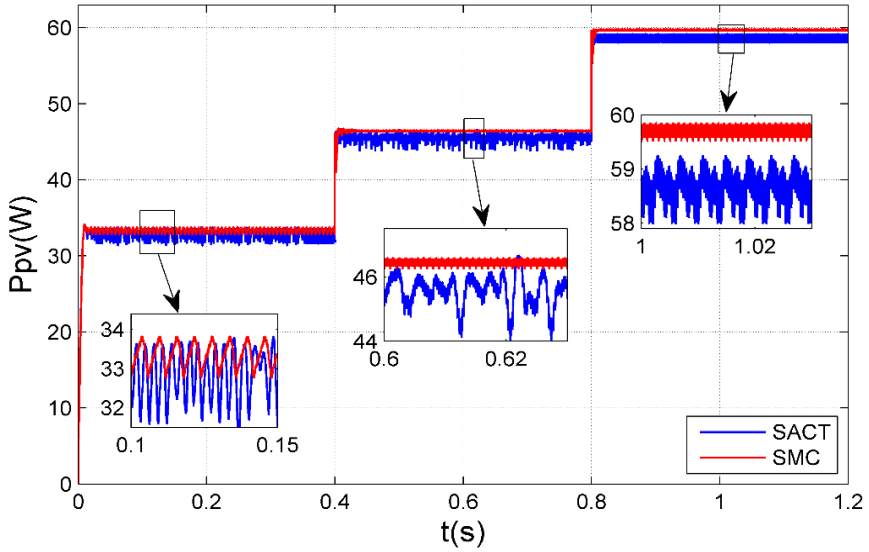

(a) The Power of PV panel

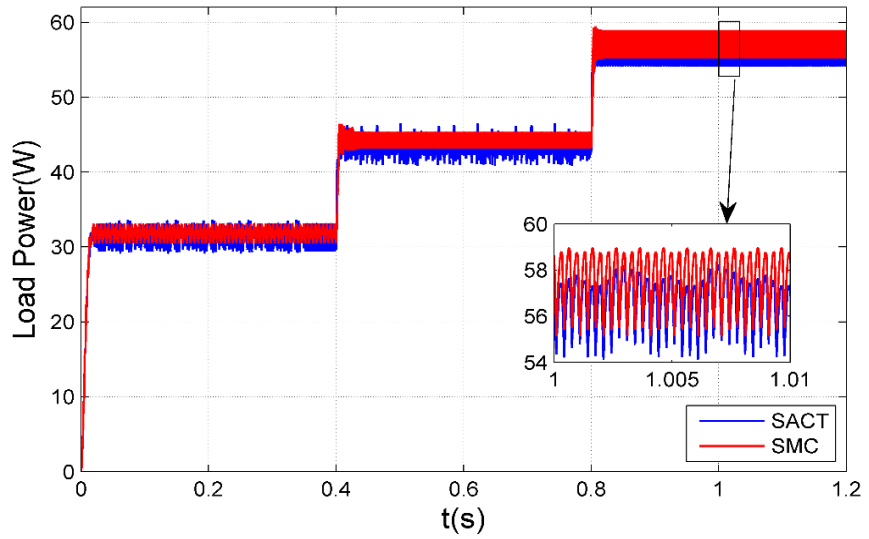

(b) The load power

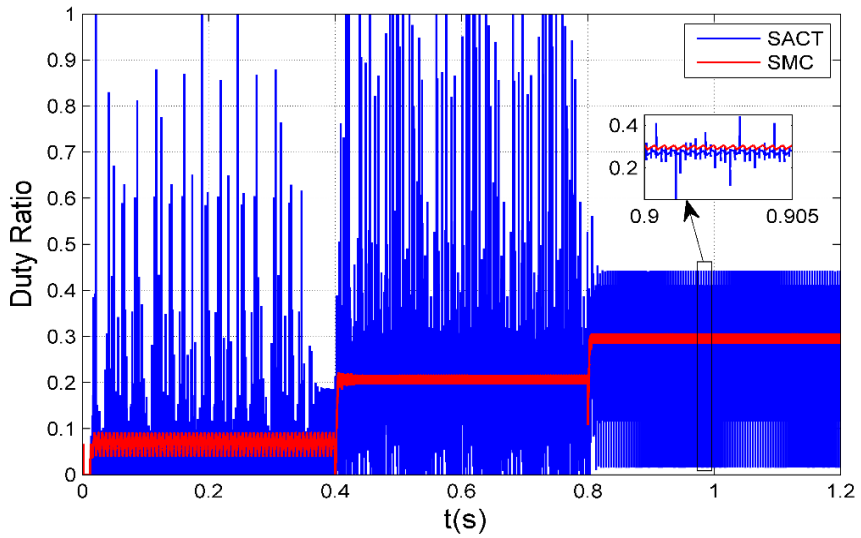

(c) The duty ratio

Fig. 8. Dynamic response of MPPT under variable irradiation conditions

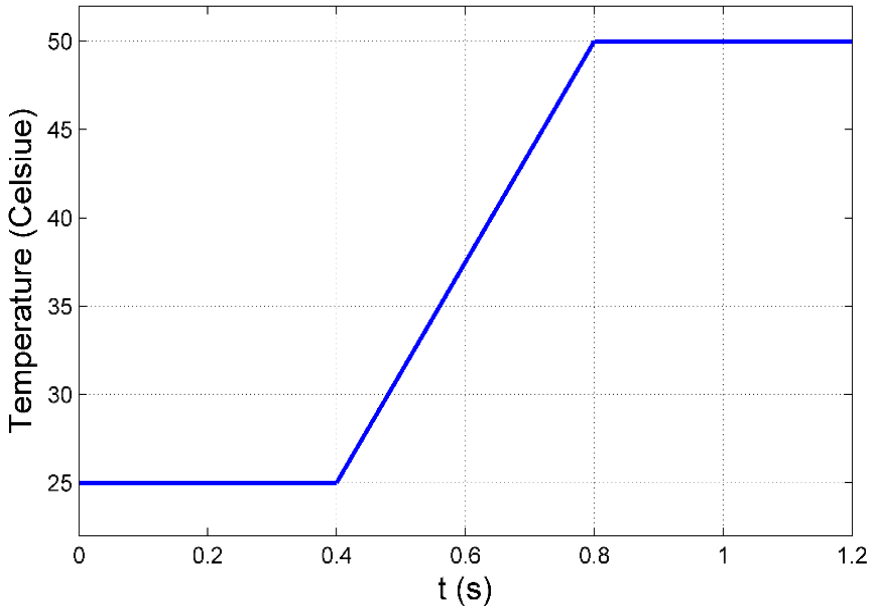

Fig. 9. Variation of temperature level

A Comparison of efficiency of a PV system using proposed MPPT methods is shown in Table 2. The results from Table 2 show that the SMC has a better performance than the SACT. For example, in the standard conditions, the PV system's tracking efficiency is increased form 97.86% in the case of SACT into 99.5% in the case of SMC. Moreover, under variable irradiation conditions scenario, the PV system's tracking efficiency is increased form 96.19% in the case of SACT into 97.68% in the case of SMC for state 1. In the same way for state 2, the PV system's tracking efficiency is increased form 97.14% in the case of SACT into 99.04% in the case of SMC. For state 3, the PV system's tracking efficiency is increased form 97.8% in the case of SACT into 99.5% in the case of SMC. In addition, under variable temperature conditions scenario, the PV system's tracking efficiency is increased form 97.85% in the case of SACT into 99.5% in the case of SMC for state 1. In the same way for state 2, the PV system's tracking efficiency is increased form 98.4% in the case of SACT into 99.4% in the case of SMC. The obtained simulation results show the outstanding performance of SMC in stabilizing the boost converter's operation compared to SACT. The operational stability of the boost converter based on SMC enhanced the tracking

efficiency of PV system, which led to a reduction in power losses. Moreover, the duty ratio produced by SMC indicates less fluctuation compared to SACT. This has led to a decrease in system oscillations around MPP.

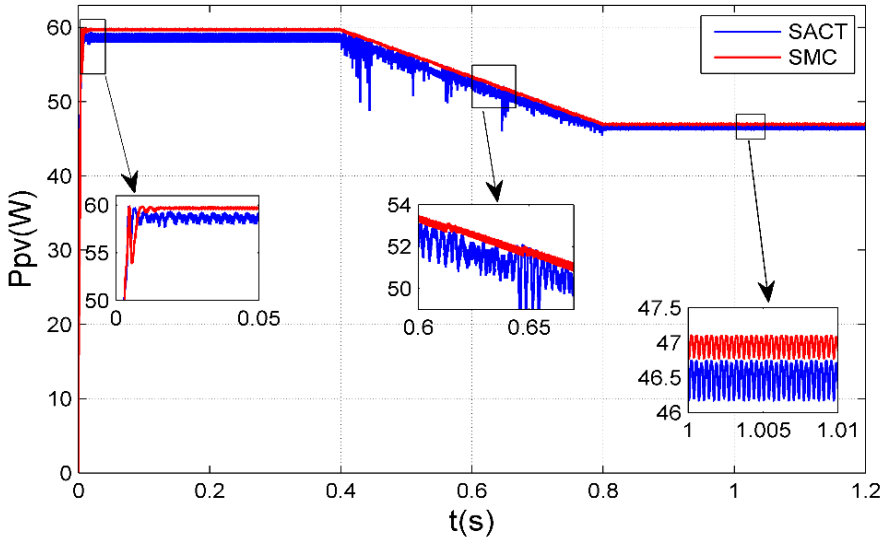

(a) The Power of PV panel

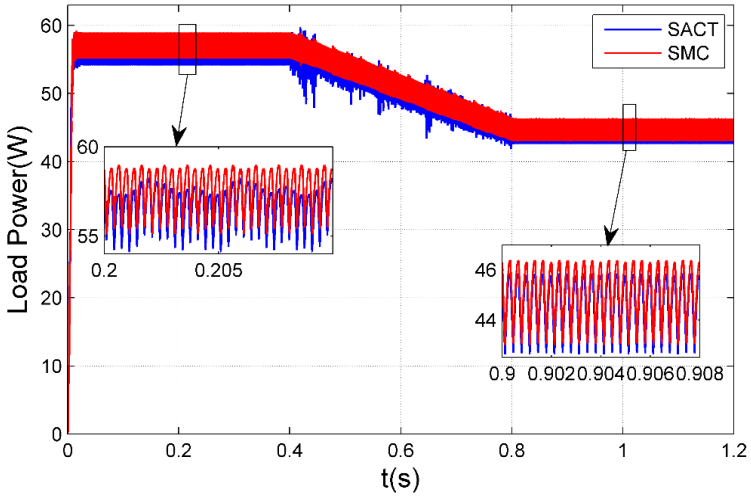

(b) The load power

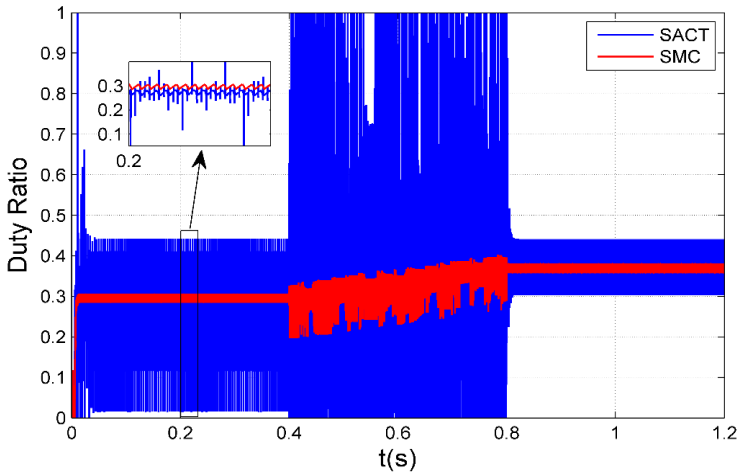

(c) The duty ratio

Fig. 10. Dynamic response of the proposed MPPT schemes under variable temperature conditions

Table 2. Accuracy of proposed MPPT schemes

Under Standard Test Conditions ($T = 25$ ℃ and $G = 1000$ W/m^2)							
State	**P(mpp)**	**(Ppv)avg**		**(Po)avg**		**η**	
		SMC	**SACT**	**SMC**	**SACT**	**SMC**	**SACT**
STC	60	59.72	58.72	57.52	56.53	99.5%	97.86%
Under Variable Irradiation Conditions							
State	**P(mpp)**	**(Ppv)avg**		**(Po)avg**		**η**	
		SMC	**SACT**	**SMC**	**SACT**	**SMC**	**SACT**
State 1 $G = 600$ W/m^2	34.13	33.34	32.83	31.87	31.37	97.68%	96.19%
State 2 $G = 800$ W/m^2	46.88	46.43	45.54	44.53	43.67	99.04%	97.14%
State 3 $G = 1000$ W/m^2	60	59.71	58.7	57.49	56.52	99.5%	97.8%
Under Variable Temperature Conditions							
State	**P(mpp)**	**(Ppv)avg**		**(Po)avg**		**η**	
		SMC	**SACT**	**SMC**	**SACT**	**SMC**	**SACT**
State 1 $T = 25$ ℃	60	59.72	58.71	57.56	56.58	99.5%	97.85%
State 2 $T = 50$ ℃	47.24	46.96	46.49	45.05	44.6	99.4%	98.4%

6. Conclusion

Maximum power point tracking (MPPT) technologies are of great importance because of their impact on the maximum energy extraction from PV. In this study, sliding mode control (SMC) and synergetic control (SACT) were used to enhance the MPPT performance of a PV system. The robustness and effectiveness of the proposed controllers were validated through numerous simulation tests conducted under various environmental conditions. The environmental conditions are one scenario under standard conditions, three scenarios under variable irradiation conditions and two scenarios under variable temperature conditions. In the standard conditions scenario, the results show that efficiency of the MPPT is increased form 97.86% (SACT) into 99.5% (SMC). Under the three variable irradiation condition scenarios, the efficiency is increased form 96.19%, 97.14% and 97.8% (SACT) into 97.68%, 99.04% and 99.5% (SMC) respectively. Under the two variable temperature condition scenarios, the efficiency is increased form 97.85% and 98.4% (SACT) into 99.5% and 99.4% (SMC) respectively. According to these results of the simulation, SMC yielded better tracking efficiency and superior robustness against variations in environmental conditions compared to SACT. The results also illustrate that SMC converges to the MPP faster than SACT, with reduced oscillations around it. Future work will focus on the practical implementation of the suggested control techniques to validate their effectiveness. Another extension of this study could be by applying a hybrid nonlinear controller such as backstepping sliding mode control.

Author Contribution: All authors contributed equally to the main contributor to this paper. All authors read and approved the final paper.

Funding: This research received no external funding.

Conflicts of Interest: The authors declare no conflict of interest.

References

[1] G. Dileep, S. N. Singh, "Maximum power point tracking of solar photovoltaic system using modified perturbation and observation method," *Renewable and Sustainable Energy Reviews*, vol. 50, pp. 109-129, 2015, https://doi.org/10.1016/j.rser.2015.04.072.

[2] U. Yilmaz, A. Kircay, S. Borekci, “PV system fuzzy logic MPPT method and PI control as a charge controller,” *Renewable and Sustainable Energy Reviews*, vol. 81, pp. 994-1001, 2018, https://doi.org/10.1016/j.rser.2017.08.048.

[3] N. S. M. N. Izam, Z. Itam, W. L. Sing, A. Syamsir, "Sustainable Development Perspectives of Solar Energy Technologies with Focus on Solar Photovoltaic-A Review," *Energies*, vol. 15, no. 8, p. 2790, 2022, https://doi.org/10.3390/en15082790.

[4] A. F. Challoob, N. A. Bin Rahmat, V. K. Ramachandaramurthy, N. Saeed and A. J. Humaidi, "An Intelligent Battery Management System for an Electric Vehicle Powered by Solar PV Array," *2024 59th International Universities Power Engineering Conference (UPEC)*, pp. 1-6, 2024, https://doi.org/10.1109/UPEC61344.2024.10892594.

[5] M. G. M. Abdolrasol, A. Ayob, A. H. Mutlag, T. S. Ustun, “Optimal fuzzy logic controller based PSO for photovoltaic system,” *Energy Reports*, vol. 9, pp. 427-434, 2023, https://doi.org/10.1016/j.egyr.2022.11.039.

[6] H. Al-Khazraji, W. Guo, and A. J. Humaidi, "Improved cuckoo search optimization for production inventory control systems," *Serbian Journal of Electrical Engineering*, vol. 21, no. 2, pp. 187-200, 2024, https://doi.org/10.2298/SJEE2402187A.

[7] F. R. Yaseen and H. Al-Khazraji, "Optimized Vector Control Using Swarm Bipolar Algorithm for Five-Level PWM Inverter-Fed Three-Phase Induction Motor," *International Journal of Robotics and Control Systems*, vol. 5, no. 1, pp. 333-347, 2025, https://doi.org/10.31763/ijrcs.v5i1.1713.

[8] A. E. Korial, I. I. Gorial, “System analysis and controllers performance comparison for DC motor,” *International Journal of Mechanical Engineering and Robotics Research*, vol. 11, no. 7, pp. 520-526, 2022, https://doi.org/10.18178/ijmerr.11.7.520-526.

[9] R. M. Naji, H. Dulaimi, and H. Al-Khazraji, "An optimized PID controller using enhanced bat algorithm in drilling processes," *Journal Européen des Systèmes Automatisés*, vol. 57, no. 3, pp. 767-772, 2024, https://doi.org/10.18280/jesa.570314.

[10] M. Q. Kadhim, F. R. Yaseen, H. Al-Khazraji and A. J. Humaidi, "Application of Terminal Synergetic Control Based Water Strider Optimizer for Magnetic Bearing Systems," *Journal of Robotics and Control (JRC)*, vol. 5, no. 6, pp. 1973-1979, 2024, https://doi.org/10.18196/jrc.v5i6.23867.

[11] N. A. Tuan and H. P. H. Anh, “Enhanced Adaptive Neuro Sliding Mode Controller Parameter Optimization for Coupled Tank System,” *Journal of Robotics and Control (JRC)*, vol. 6, no. 3, pp. 1293-1307, 2025, https://doi.org/10.18196/jrc.v6i3.25992.

[12] F. R. Yaseen, M. Q. Kadhim, H. Al-Khazraji and A. J. Humaidi, "Decentralized Control Design for Heating System in Multi-Zone Buildings Based on Whale Optimization Algorithm," *Journal Européen des Systèmes Automatisés*, vol. 57, no. 4, pp. 981-989, 2024, https://doi.org/10.18280/jesa.570406.

[13] H. Maghfiroh *et al*., “Induction Motor Speed Control Using PID Tuned by Particle Swarm Optimization Under Vector Control,” *Buletin Ilmiah Sarjana Teknik Elektro*, vol. 7, no. 2, pp. 172-180, 2025, https://doi.org/10.12928/biste.v7i2.13112.

[14] F. R. Al-Ani, O. F. Lutfy, H. Al-Khazraji, "Optimal Backstepping and Feedback Linearization Controllers Design for Tracking Control of Magnetic Levitation System: A Comparative Study," *Journal of Robotics and Control (JRC)*, vol. 5, no. 6, pp. 1888-1896, 2024, https://doi.org/10.18196/jrc.v6i1.24452.

[15] S. A. Al-Samarraie, I. I. Gorial, “Modeling of electromechanical system and motion control for mechatronics application,” *International Review of Automatic Control*, vol. 16, no. 5, pp. 246-252, 2023, https://doi.org/10.15866/ireaco.v16i5.24226.

[16] M. A. Al-Ali, O. F. Lutfy, H. Al-Khazraj, "Investigation of Optimal Controllers on Dynamics Performance of Nonlinear Active Suspension Systems with Actuator Saturation," *Journal of Robotics and Control (JRC)*, vol. 5, no. 4, pp. 1041-1049, 2024, https://doi.org/10.18196/jrc.v5i4.22139.

[17] M. Nawfal, A. A. Yahya, R. A. Mahmod, H. Al-Khazraji, "Integration of Sparrow Search Optimization with Terminal Synergetic Control for Permanent Magnet Linear Synchronous Motors," *Journal of*

Robotics and Control (JRC), vol. 6, no. 2, pp. 1033-1040, 2025, https://doi.org/10.18196/jrc.v6i2.26174.

[18] R. Al-Majeez, K. Al-Badri, H. Al-Khazraji, S. M. Ra'afat, "Design of A Backstepping Control and Synergetic Control for An Interconnected Twin-Tanks System: A Comparative Study," *International Journal of Robotics and Control Systems*, vol. 4, no. 4, pp. 2041-2054, 2024, https://doi.org/10.31763/ijrcs.v4i4.1682.

[19] P. Das, "Maximum Power Tracking Based Open Circuit Voltage Method for PV System," *Energy Procedia*, vol. 90, pp. 2-13, 2016, https://doi.org/10.1016/j.egypro.2016.11.165.

[20] R. M. Asif *et al*., "Design and analysis of robust fuzzy logic maximum power point tracking based isolated photovoltaic energy system," *Engineering Reports*, vol. 2, no. 9, p. e12234, 2020, https://doi.org/10.1002/eng2.12234.

[21] R. S. Sharma and P. K. Katti, "Perturb & observation MPPT algorithm for solar photovoltaic system," *2017 International Conference on Circuit, Power and Computing Technologies (ICCPCT)*, pp. 1-6, 2017, https://doi.org/10.1109/ICCPCT.2017.8074191.

[22] D. Guiza, D. Ounnas, Y. Soufi, A. Bouden and M. Maamri, "Implementation of Modified Perturb and Observe Based MPPT Algorithm for Photovoltaic System," *2019 1st International Conference on Sustainable Renewable Energy Systems and Applications (ICSRESA)*, pp. 1-6, 2019, https://doi.org/10.1109/ICSRESA49121.2019.9182483.

[23] R. I. Putri, S. Wibowo, and M. Rifa'i, "Maximum power point tracking for photovoltaic using incremental conductance method," *Energy Procedia*, vol. 68, pp. 22-30, 2015, https://doi.org/10.1016/j.egypro.2015.03.228.

[24] H. T. Yau and C. H. Wu, "Comparison of extremum-seeking control techniques for maximum power point tracking in photovoltaic systems," *Energies*, vol. 4, no. 12, pp. 2180-2195, 2011, https://doi.org/10.3390/en4122180.

[25] P. Cheng, B. Peng, Y. Liu, Y. Cheng, and J. Huang, "Optimization of a fuzzy-logic-control-based MPPT algorithm using the particle Swarm optimization technique," *Energies*, vol. 8, no. 6, pp. 5338-5360, 2015, https://doi.org/10.3390/en8065338.

[26] K. Kayisli, "Super twisting sliding mode-type 2 fuzzy MPPT control of solar PV system with parameter optimization under variable irradiance conditions," *Ain Shams Engineering Journal*, vol. 14, no. 1, p. 101950, 2023, https://doi.org/10.1016/j.asej.2022.101950.

[27] K. Dahech, M. Allouche, T. Damak, and F. Tadeo, "Backstepping sliding mode control for maximum power point tracking of a photovoltaic system," *Electric Power Systems Research*, vol. 143, pp. 182-188, 2017, https://doi.org/10.1016/j.epsr.2016.10.043.

[28] A. Kihal, F. Krim, A. Laib, B. Talbi, and H. Afghoul, "An improved MPPT scheme employing adaptive integral derivative sliding mode control for photovoltaic systems under fast irradiation changes," *ISA Transactions*, vol. 87, pp. 297-306, 2019, https://doi.org/10.1016/j.isatra.2018.11.020.

[29] A. Q. Al-Dujaili, A. J. Humaidi, Z. T. Allawi, and M. E. Sadiq, "Earthquake hazard mitigation for uncertain building systems based on adaptive synergetic control," *Applied System Innovation*, vol. 6, no. 2, p. 34, 2023, https://doi.org/10.3390/asi6020034.

[30] V. Utkin, J. Guldner, J. Shi, "Sliding mode control in electro-mechanical systems," *CRC press*, 2017, https://books.google.co.id/books?id=8IrLBQAAQBAJ&source=gbs_navlinks_s.

[31] A. Ma'arif, M. A. M. Vera, M. S. Mahmoud, E. Umoh, A. J. Abougarair, and S. N. Rahmadhia, "Sliding Mode Control Design for Magnetic Levitation System," *Journal of Robotics and Control (JRC)*, vol. 3, no. 6, pp. 848-853, 2023, https://doi.org/10.18196/jrc.v3i6.12389.

[32] Z. A. Waheed, A. J. Humaidi, "Design of Optimal Sliding Mode Control of Elbow Wearable Exoskeleton System Based on Whale Optimization Algorithm," *Journal Européen des Systèmes Automatisés*, vol. 55, no. 4, pp. 459-466, 2022, https://doi.org/10.18280/jesa.550404.

[33] H. Al-Khazraji, K. Al-Badri, R. Almajeez, and A. J. Humaidi, "Synergetic control-based sea lion optimization approach for position tracking control of ball and beam system," *International Journal of*

Robotics and Control Systems, vol. 4, no. 4, pp. 1547-1560, 2024, https://doi.org/10.31763/ijrcs.v4i4.1551.

[34] H. Al-Khazraji, K. Al-Badri, R. Al-Majeez, and A. J. Humaidi, "Synergetic Control Design Based Sparrow Search Optimization for Tracking Control of Driven-Pendulum System," *Journal of Robotics and Control (JRC)*, vol. 5, no. 5, pp. 1549-1556, 2024, https://doi.org/10.18196/jrc.v5i5.22893.

[35] F. R. Al-Ani, O. F. Lutfy, and H. Al-Khazraji, "Optimal Synergetic and Feedback Linearization Controllers Design for Magnetic Levitation Systems: A Comparative Study," *Journal of Robotics and Control (JRC)*, vol. 6, no. 1, pp. 22-30, 2025, https://doi.org/10.18196/jrc.v6i1.24452.

[36] R. D. Silveira, G. P. das Neves, S. A. O. da Silva, and B. A. Angélico, "An enhanced MPPT algorithm based on adaptive extremum-seeking control applied to photovoltaic systems operating under partial shading," *IET Renewable Power Generation*, vol. 15, no. 6, pp. 1227-1239, 2021, https://doi.org/10.1049/rpg2.12102.

[37] A. Gupta, Y. K. Chauhan, and R. K. Pachauri, "A comparative investigation of maximum power point tracking methods for solar PV system," *Solar Energy*, vol. 136, pp. 236-253, 2016, https://doi.org/10.1016/j.solener.2016.07.001.

[38] J. Hahm, J. Baek, H. Kang, H. Lee, and M. Park, "Matlab-based modeling and simulations to study the performance of different MPPT techniques used for photovoltaic systems under partially shaded conditions," *International Journal of Photoenergy*, vol. 2015, no. 1, pp. 1-11, 2015, https://doi.org/10.1155/2015/979267.

[39] S. D. Al-Majidi, M. F. Abbod, and H. S. Al-Raweshidy, "A novel maximum power point tracking technique based on fuzzy logic for photovoltaic systems," *International Journal of Hydrogen Energy*, vol. 43, no. 31, pp. 14158-14171, 2018, https://doi.org/10.1016/j.ijhydene.2018.06.002.

[40] P. K. Pathak and A. K. Yadav, "Design of battery charging circuit through intelligent MPPT using SPV system," *Solar Energy*, vol. 178, pp. 79-89, 2019, https://doi.org/10.1016/j.solener.2018.12.018.

[41] R. A. M. Lameirinhas, J. P. N. Torres, and J. P. d. M. Cunha, "A Photovoltaic Technology Review: History, Fundamentals and Applications," *Energies*, vol. 15, no. 5, p. 1823, 2022, https://doi.org/10.3390/en15051823.

[42] E. Nechadi, M. N. Harmas, N. Essounbouli, and A. Hamzaoui, "Optimal Synergetic Control based Bat Algorithm for DC-DC Boost Converter," *IFAC-PapersOnLine*, vol. 49, no. 12, pp. 698-703, 2016, https://doi.org/10.1016/j.ifacol.2016.07.792.

[43] A. F. Mutlak, A. J. Humaidi, "A Comparative Study of Synergetic and Sliding Mode Controllers for Pendulum Systems," *Journal Européen des Systèmes Automatisés*, vol. 56, no. 5, pp. 871-877, 2023, https://doi.org/10.18280/jesa.560518.

[44] A. K. Abbas, S. K. Kadhim, "Eliminating Chattering in Prosthetic Fingers Using Classic Synergetic Control," *Journal Européen des Systèmes Automatisés*, vol. 58, no. 1, pp. 75-87, 2024, https://doi.org/10.18280/jesa.580109.

[45] S. M. Mahdi, N. Q. Yousif, A. A. Oglah, M. E. Sadiq, A. J. Humaidi, and A. T. Azar, "Adaptive synergetic motion control for wearable knee-assistive system: a rehabilitation of disabled patients," *Actuators*, vol. 11, no. 7, p. 176, 2022, https://doi.org/10.3390/act11070176.

[46] A. F. Mutlak and A. J. Humaidi, "Adaptive synergetic control for electronic throttle valve system," *International Review of Applied Sciences and Engineering*, vol. 15, no. 2, pp. 211-220, 2024, https://doi.org/10.1556/1848.2023.00706.

[47] M. Mahmoud, R. Saleh, A. Ma'arif, "Stabilizing of inverted pendulum system using Robust sliding mode control," *International Journal of Robotics and Control Systems*, vol. 2, no. 2, pp. 230-239, 2022, https://doi.org/10.31763/ijrcs.v2i2.594.

[48] S. A. Al-Samarraie and I. I. Gorial, "Assessment of FLC, PID, Nonlinear PID, and SMC controllers for level stabilization in mechatronic systems," *Journal of Robotics and Control (JRC)*, vol. 5, no. 6, pp. 1845-1861, 2024, https://doi.org/10.18196/jrc.v5i6.23639.

[49] D. S. Shanan, S. K. Kadhim, "Comparative Analysis of Airflow Regulation in Ventilator Systems Using Various Control Strategies," *Journal Européen des Systèmes Automatisés*, vol. 56, no. 5, pp. 811-821, 2023, https://doi.org/10.18280/jesa.560512.

[50] S. A. AL-Samarraie and S. D. Salman, "Backstepping Nonlinear Control for Blood Glucose Based on Sliding Mode Meal Observer," *Al-Nahrain Journal for Engineering Sciences*, vol. 21, no. 3, pp. 436-444, 2018, https://doi.org/10.29194/NJES.21030436.

[51] H. T. Yau and C. Chen, "Fuzzy sliding mode controller design for maximum power point tracking control of a solar energy system," *Transactions of the Institute of Measurement and Control*, vol. 34, no. 5, pp. 557-565, 2012, https://doi.org/10.1177/0142331211407959.